Turk J Chem
34 (2010) , 437 – 445.

doi:10.3906/kim-0907-140

Synthesis and characterization of hybrid congo red from chloro-functionalized silsesquioxanes

Ahmet GÜLTEK
İnönü University, Department of Chemistry, Malatya, 44280, TURKEY
e-mail: agultek@inonu.edu.tr

Received 18.07.2009

Congo red dye has been bonded to the functionalized octameric polyhedral silsesquioxanes (POSS), which were prepared by hydrolytic condensation of chloro-functionalized organosilicon monomers in the presence of a catalyst. The binding reaction of congo red to the POSS with chloro groups was achieved via the addition of the congo red via NaCl elimination. The structures of POSS with chloro side groups provided an attractive site for binding congo red that not only retains some of its characteristic properties, but also has exceptional hybrid properties possessed by the silica. The dye characteristics of the material were determined by means of UV spectroscopy as well as other conventional techniques.

Key Words: Ceramic dye, hybrid dye, POSS, congo red.

Introduction

The azo dye congo red has a high affinity with the β-pleated structure of all forms of amyloid.[1] Unfortunately, it is also known as mutagenic in the preincubation assay. The mutogenicity of congo red has been attributed to the generation of benzidine, via metabolic activation, a compound known to cause cancer in humans.[2] More recently the amyloid protein binding capacity of congo red was attributed to its symmetrical structure and the separation of negatively charged groups.[2]

The present investigation focuses on the preparation of hybrid congo red with the development of a polyhedral oligomeric silsesquioxane (POSS) framework by the sol-gel process in which the symmetrical structure of congo red and its charge separation were prevented by introducing the silica cage (POSS) by forming a novel hybrid congo red pigment.

While several processes for the production of a POSS framework or nano particles derived from the POSS technology have appeared in recent studies, these applications are constrained by the necessity of providing binding sites for the pigment and its characterization.

One of the most extensively studied systems, involving the preparation of polyhedral oligomeric silsesquioxane, is their derivative. The results of experimental and theoretical studies of these systems suggest that the morphology is governed by 3 effects: the type of the organosilane, the solvent, and the catalyst.[3–28]

While the first 2 effects are now usually taken into account in both experimental and theoretical studies, the literature dealing with the process conditions remains very scarce, mainly because of the lack of experimental data on the process conditions of well-controlled morphology. In this work, I try partially to fill this gap by giving a method of preparation of the POSS molecules from γ-chloropropyltrimethoxy silane (CLS) by the sol-gel process in the presence of a catalyst. In this work our objective is 3-fold: (1) to give the experimental conditions to prepare the POSS molecules; (2) to elucidate the structure by means of X-ray diffraction (XRD) studies, Fourier transform infrared spectroscopy (FT-IR), and ^{13}C and ^{1}H nuclear magnetic resonance (NMR) spectroscopy; (3) to prepare nano particular congo red POSS molecules from CLS.

Experimental

Materials and methods

All reactions were performed under an atmosphere of dry nitrogen using standard Schlenk techniques. Solvents and chemicals were obtained from Aldrich and used as received unless specified otherwise. Congo red (CR) was used as received since the dye content was verified to be 97%. An ultra-pure water filtering system was used to produce deionized water, and methanol was dried over calcium hydride.

Infrared spectra were recorded as KBr pellets in the range 4000-400 cm^{-1} on an ATI UNICAM systems 2000 Fourier transform spectrometer. ^{1}H-NMR spectra (300 MHz) and ^{13}C-NMR spectra (75.5 MHz) were recorded on a Bruker AM 300 WB FT spectrometer with δ referenced to residual solvent $CDCl_3$. Differential scanning calorimetry (DSC), differential thermal analysis (DTA), and thermogravimetry (TG) were performed with Shimadzu DSC-60, DTA-50, and TGA-50 thermal analyzers, respectively.

Gel permeation chromatography (GPC) analyses were performed at 30 °C using N-methyl-2-pyrolidone (NMP) as eluant at a flow rate of 0.5 mL/min. A differential refractometer was used as a detector. The instrument (Agilent 1100 series GPC-SEC system) was calibrated with a mixture of polystyrene standards (Polysciences; molecular masses 200-1,200,000 Da) using GPC software for the determination of the average molecular masses and the polydispersity of the samples.

Preparation of octa-γ-chloropropyloctasilsesquioxane (POSS-CLS)

In each sol-gel polymerization, the monomer solutions and the monomer and catalyst solutions (200 ppm by weight) were sealed in polypropylene bottles, the product was washed with H_2O (3 × 100 mL) and ether (2 × 50 mL), and dried under vacuum for 24 h at 100 °C.

A solution of 3-chloropropyltrimethoxysilane (CLS) (45 mL) was added to a solution of dry methanol. To this mixture was added 28 mL of concentrated HCl, and the reaction mixture was kept at room temperature for 2 days. $PtCl_4$ was added to this solution as catalyst in an argon atmosphere. The reaction mixture was transferred to the Schlenk tube and heated to 50 °C. A crystalline precipitate formed after a day at 50 °C, which was collected and treated as described above. The product has a melting point of 207 °C and the chlorine

content was found to be 27.6%. The GPC chromatogram indicated a monodisperse compound. The product, obtained in 45% yield, was filtered, and washed with cold methanol and dried in a vacuum oven at 30 °C. The ^{1}H-NMR and ^{13}C-NMR (DMSO-d_6): 1.98 (m, $SiCH_2CH_2CH_2CH_2$, 16H), 0.98 (m, $SiCH_2CH_2CH_2CH_2$, 16H), 3.78 (m, $SiCH_2CH_2CH_2CH_2$, 16H), (DMSO-d_6): 51.2 (s, $SiCH_2CH_2CH_2CH_2$), 19.4 (s, $SiCH_2CH_2CH_2CH_2$) 14.2 (s, $SiCH_2CH_2CH_2CH_2$).

Procedure for binding of congo red to POSS-CLS

Congo red (Aldrich, 0.624 g, 0.9 mmol) and POSS-CLS (14.8, 14.34 mmol) were reacted for 48 h in refluxing DMSO (25 mL). The yield was quantitated by ^{1}H- and ^{13}C-NMR spectroscopy. Upon cooling hybrid dye crystallized as red crystals (80% wt). The solid particles were collected by filtration and extracted with methanol and dichloromethane in a Soxhlet apparatus for 24 h to remove unreacted dye molecules that were physically adsorbed. The samples were then dried in a vacuum at 110 °C for 2 h.

Sample preparation for UV

Sample was first dispersed in ethylene glycol and the dispersion was subsequently stirred for 5 h. The solutions were allowed to cool down and the desired concentration was adjusted by dilution. Measurements were performed with the use of a Shimadzu UV-1601 spectrometer.

Results and discussion

Octafunctional octahedral silsesquioxanes $[RSiO_{1.5}]_8$ (POSS) or cubic silsesquioxanes $[RSiMe_2OSiO_{1.5}]_8$ (cubes) represent 3-dimensional nanobuilding blocks. Polyhedral oligomeric silsesquioxanes $(RSiO_{1.5})_{2n}$ (n = 2, 3, 4) have attracted considerable interest in the last few years. They are accessible by hydrolysis of trifunctional $RSiY_3$ molecules and can be modified by a number of substitution reactions. Thus, functionalized silsesquioxanes have become available, which are interesting as precursors to organolithic macromolecular materials or hybrid inorganic–organic materials. They have become prevalent during the past decade for use in preparing organic-inorganic hybrid materials with precise control tailoring of the nanoarchitecture and their properties can be tailored. Congo red dye has been tailored to the prepared POSS framework as shown in Figure 1.

The application of hybrid dye in imaging techniques has become an area of intense interest because of the potential environmental advantages related to recoverability, handling, recycling, and expense. In addition, the use of hybrid dye can lead to isomerically pure products, which are especially important in the production of radiopharmaceuticals.[29–38]

The azo dye congo red has been used in nuclear medicine imaging techniques by localizing β-amyloid fibrils, and it might be possible to monitor in vivo levels of amyloid by single photon emission computerized tomographic imaging.[39,40] Hybrid congo red (POSS-CLS-CR) can easily be used to form radiopharmaceuticals by isolation without showing any toxicity due to its cage structure, which prevents benzidine formation.

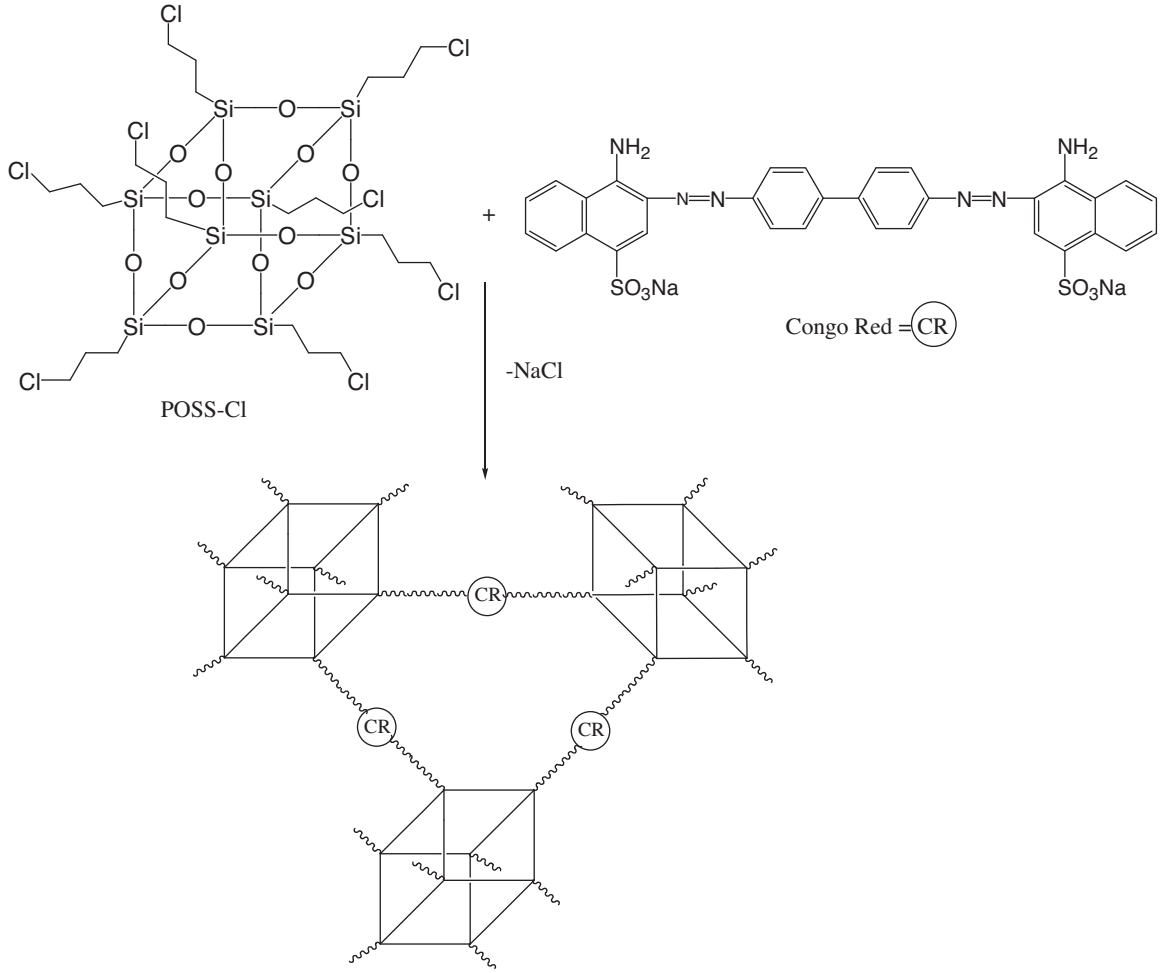

Figure 1. Synthesis route for the preparation of POSS-CLS-CR hybrid dye.

Figure 2 shows the DTA curves of hybrid dye, congo red, and the POSS-CLS-CR recorded in air atmosphere. The temperature range of each peak and the maxima of the exothermic peaks demonstrate the thermal behavior of the hybrid dye. All these curves can be divided into 3 regions: the dehydration below 200 °C, the region of combustion reaction up to 400-550 °C represented by 2 exothermic peaks, and the decomposition peak over 600 °C.

As shown in Figure 2, the exothermic peak temperature of 329 °C corresponds to the loss of organic segments, whereas the exothermic peaks temperatures of 432 and 535 °C are attributed to the phase transition temperatures in CR, the peak of 207 °C corresponds the loss of organic segments, and the peak of 425 °C corresponds to the phase transition in POSS-CLS. For POSS-CLS-CR, the peaks of 278 and 437 °C were attributed to the loss of organic segment, whereas the peak of 569 °C corresponds to the phase transition in the hybrid dye. All evidence was supported by TGA analysis. The difference in peak temperature is due to the molecular symmetry, and molecular rearrangement is more likely to take place.

The FT-IR spectra of both frameworks are shown in Figure 3. The tentative assignments for the spectra of the framework were as follows: 1174 cm^{-1} (asymmetrical) ν_{as} (Si-O-Si), 1060 cm^{-1} ν (Si-O-), 938 and

785 cm^{-1} (symmetrical) ν_s(Si-O-Si), 620 and 550 $cm^{-1}\nu_s$ (Si-O-Si). Polysiloxanes made up tetrahedral (T) units, $[RSiO_{1.5}]_x$, and showed a broad, structureless absorption covering the entire region of 1160-1000 cm^{-1}. The bands observed at 1630, 1280, and 1155 cm^{-1} indicated aromatic C=C vibration, symmetric stretching of S=O, and asymmetric stretching of S=O. However, FT-IR spectra of hybrid dye indicated the formation of linkage between $SO_3^-Na^+$ groups and amino groups on the CR molecule.

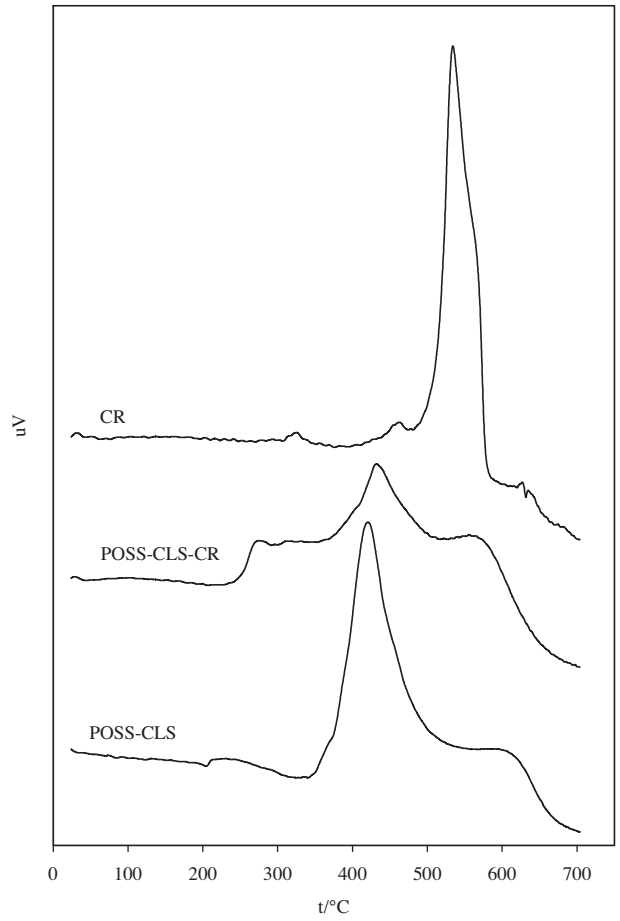

Figure 2. DTA spectra of congo red (CR), POSS-CLS, and the hybrid pigment (POSS-CLS-CR) with a heating rate of 10 °C/min in air.

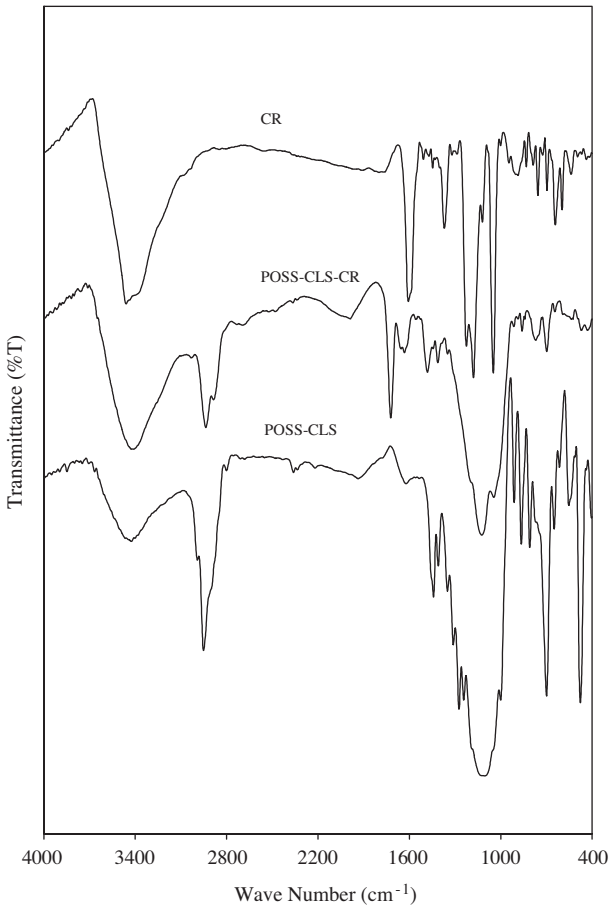

Figure 3. FT-IR spectra of congo red (CR), POSS-CLS, and the hybrid pigment (POSS-CLS-CR).

Figure 4 shows the ultraviolet absorption spectra of CR, POSS-CLS, and the hybrid dye POSS-CLS-CR in ethylene glycol. The maximum at 532 nm in the spectra of CR in the hybrid diminished. This fact suggests the formation of a complex between POSS frame and CR molecules. CR is known to show a blue shift when it binds to cellulose fibers or amyloid fibrils.[41] The UV spectrum of CR in aqueous solution shifts ∼26 nm to smaller wavelengths in the presence of CTAB.[41] When CR was incorporated in Langmuir-Blodgett films of CTAB and stearic acid, the UV peak at 532 nm diminished completely as in the POSS-CLS-CR case. I thus conclude that the absence of the 532 nm peak indicates the successful formation of POSS-CLS-CR.

The XRD patterns of POSS-CLS and POSS-CLS-CR are shown in Figure 5. The complete lists of

observed and calculated inter-planar spacing for both frameworks are given in the Table. The observed pattern for POSS-CLS can be fitted to a hexagonal unit cell with the parameters $a = b = 16.77$ Å and $c = 17.46$ Å. The presence of a broad peak at 2 theta ∼15-30 indicates an amorphous matrix in which POSS-CLS crystallites exist. As the CR molecules can connect any 2 corners of the POSS-CLS cube, POSS-CLS-CR may not form a well-ordered structure and leads to the amorphous broad peak.

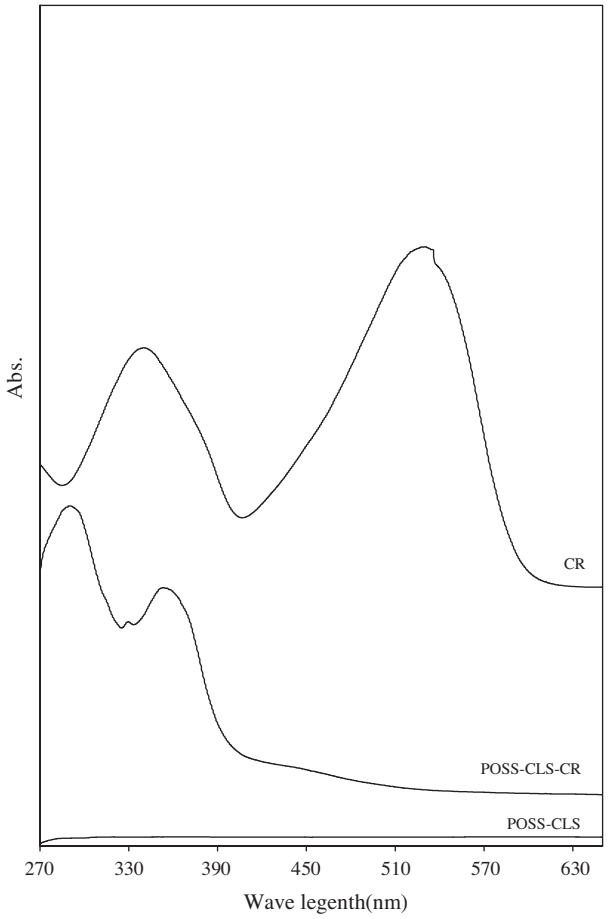

Figure 4. UV-vis spectra of congo red (CR), POSS-CLS, and the hybrid pigment (POSS-CLS-CR) in ethylene glycol at room temperature.

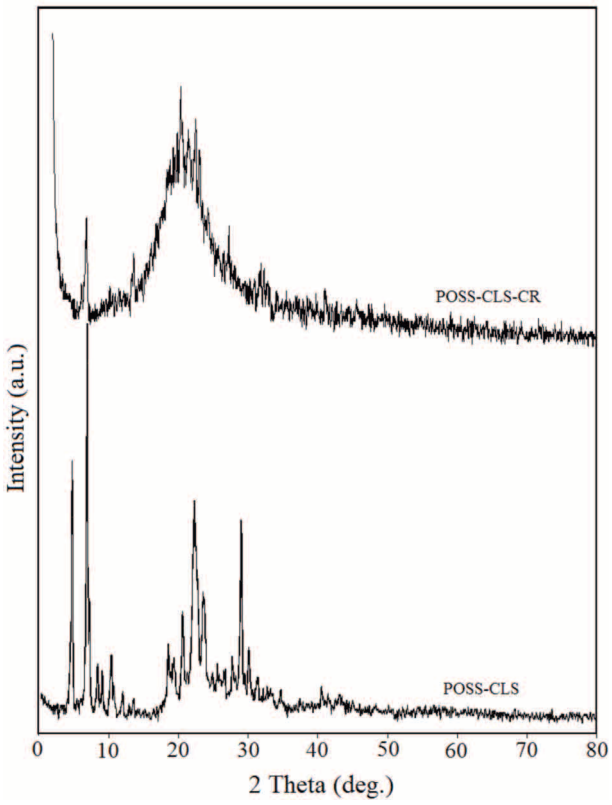

Figure 5. The X-ray powder diffraction profile of POSS-CLS and hybrid pigment (POSS-CLS-CR).

I investigated the morphologies of the CR-POSS hybrid pigment by SEM. Figure 6a and b display the SEM cross-sectional images of the POSS-CLS (a) and the hybrid pigment (POSS-CLS-CR) (b). In Figure 6a, the SEM image of the POSS-CLS indicates that the POSS moieties are still dispersed evenly. The POSS-CLS has a dense morphology and crystalline structure. For the POSS-CLS, the light gray spots of about 100-250 μm in size distributed across the dark background are probably the cubic crystalline aggregates of the POSS groups. The voids (dark spots) of about 15-20 nm in size in Figure 6a are probably associated with the external porosity, arising from the stacking of the POSS. In scanning electron micrograph images of the hybrid pigment (POSS-CLS-CR) (Figure 6b), POSS particles are homogeneously distributed in the hybrid network regularly.

CR-POSS hybrid pigment is a self-assembled system, so that nanocomposites formed by covalent bonding can be distributed in hybrid network in a way of effectively controlling polyhedral oligomeric silsesquioxane. Many crystallites with well-defined boundaries are seen in POSS-CLS, while few crystallites are seen in POSS-CLS-CR in a featureless film, consistent with the observation of a broad amorphous peak in XRD data. The POSS groups in the hybrid network are well distributed and do not aggregate. It is proposed that the nanostructuring of the CR molecular network is the result of incorporating POSS into the network as illustrated schematically in the Scheme.

Table. Observed and calculated 2θ values using a hexagonal cell with $a = b = 16.77$ Å, $c = 17.46$ Å and the measured diffraction intensity from the X-ray powder diffraction pattern obtained from POSS-CLS.

2θ obs./degrees	2θ calc./degrees	Error (%)	hkl
10.12	10.12	0	002
11.82	11.82	0	012
18.54	18.54	0	123
19.08	19.08	0	132
22.64	22.72	8	141
27.23	27.20	3	251
28.08	28.08	0	151

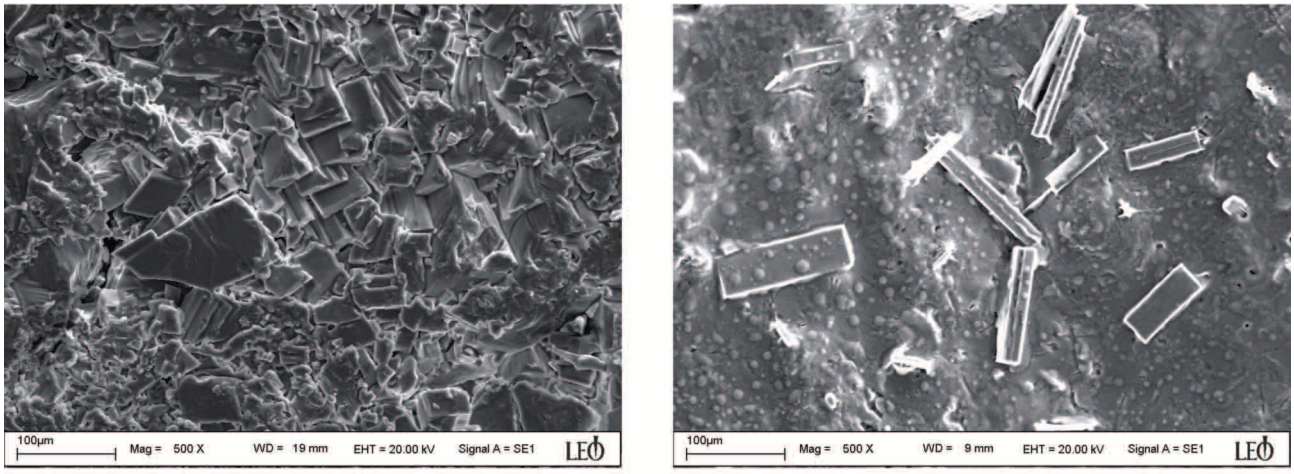

(a) (b)

Figure 6. Scanning electron micrograph images of POSS-CLS (a) and the hybrid pigment (POSS-CLS-CR) (b).

Conclusions

Efforts were made in this study towards the development of non-mutagenic form of hybrid dye to afford the beneficial properties of CR in which the benzidine moiety imparts to dyes and potential xenobiotics. The structure of the dye was changed with the introduction of silica cage based on POSS to the dye molecule, which I assume would reduce mutagenicity, while retaining the desirable dye properties.

References

1. Turnell, W. G.; Finch, J. T. *J. Mol. Biol.* **1992,** *227*, 1205-1223.
2. Prival, M. J.; Bell, S. J.; Mitchell, V. D.; Peiperl M. D.; Vaughan, V. L. *Mutattion Res./Genetic Toxicology* **1984,** *136*, 33-47.
3. Feher, F. J.; Soulivong, D.; Eklund, A. G. *Chem. Commun* **1998,** 399-400.
4. Feher, F. J.; Soulivong, D.; Nguyen, F. *Chem. Commun* **1998,** 1279-1280.
5. Feher, F. J.; Wyndham, K. D.; Knauer D. J. *Chem. Commun* **1998,** 2393-2394.
6. Feher, F. J.; Wyndham, K. D.; Scialdone, M. A.; Hamuro, Y. *Chem. Commun* **1998,** 1469-1470.
7. Feher, F. J.; Soulivong, D.; Eklund, A. G.; Wyndham, K. D. *Chem. Commun* **1997,** 1185-1186.
8. Mantz, R. A.; Jones, P. F.; Chaffe, K. P.; Lichtenhan J. D.; Gilman, J. W. *Chem. Mater.* **1996,** *8*, 1250-1259.
9. Feher, F. J.; Soulivong, D. T.; Lewis, G. T. *J. Am. Chem. Soc.* **1997,** *119*, 11323-11324.
10. Lee, A.; Lichtenhan, J. D. *Macromolecules* **1998,** *31*, 4970-4974.
11. Gültek, A.; Seçkin T.; Adıgüzel, H. İ. *Turk. J. Chem.* **2005,** *29*, 391-399.
12. Marui, A. N.; Riccardi, C. C.; Williams, R. J. J. *Poly. Bull.* **2001,** *45*, 523-530.
13. Sellinger, A.; Laine, R. M. *Chem. Mater.* **1996,** *8*, 1592-1593.
14. Feher, F. J.; Phillips, S. H.; Ziller, J. W. *J. Am. Chem. Soc.* **1997,** *119*, 3397-3398.
15. Zhang, C.; Babonneau, F.; Bonhemme, C.; Laine, R. M.; Soles, C. L.; Hristov, H. A.; Yee, A. F. *J. Am. Chem. Soc.* **1998,** *120*, 8380-8391.
16. Kudo, T.; Gordon, M. S. *J. Am. Chem. Soc.* **1998,** *120*, 11432-11438.
17. Sellinger, A.; Laine, R. M. *Macromolecules* **1996,** *29*, 2327-2330.
18. Haddad, T. S.; Lichtenhan, J. D. *Macromolecules* **1996,** *29*, 7302-7304.
19. Tsuchida, A.; Bolln, C.; Sernetz, F. G.; Frey H.; Mülhaupt, R. *Macromolecules* **1997,** *30*, 2818-2824.
20. Hedrick, J. L.; Cha, H. J.; Miller, R. D.; Yoon, D. Y.; Brown, H. R.; Srinivasan, S.; Pietro, R. D.; Cook, R. F.; Hummel, J. P.; Klaus, D. P.; Liniger, E. G.; Simonyi, E. E., *Macromolecules* **1997,** *30*, 8512-8515.
21. Lee, A.; Lichtenhan, J. D. *Macromolecules* **1998,** *31*, 4970-4974.
22. Harkness, B. R.; Takeuchi K.; Tachikawa, M. *Macromolecules* **1998,** *31*, 4798-4805.
23. Fasce, D. P.; Williams, R. J. J.; Mechin, F.; Pascault, J. P.; Llauro, M. F.; Petiaud, R. *Macromolecules* **1999,** *32*, 4757-4763.
24. Pyun, J.; Matyjaszewski, K. *Macromolecules* **2000,** *33*, 217-220.
25. Eisenberg, P.; Erra-Balsells, R.; Ishikawa, Y.; Lucas, J. C.; Mauri, A. N.; Nonami, H; Riccardi, C. C.; Williams, R. J. J. *Macromolecules* **2000,** *33*, 1940-1947.
26. Chandrasekhar, V.; Murugavel, R.; Voigt, A.; Roesky, H. W.; Schmidt, H. G.; Noltemeyer, M. *Organometallic* **1996,** *15,* 918-922.
27. Klemp, A.; Roesky, H. W.; Schmidt, H. G.; Park, H. S.; Noltemeyer, M. *Organometallics* **1998,** *17*, 5225-5227.
28. Duchateau, R.; Abbenhuis, H. C. L.; van Santen, R. A.; Thiele, S. K. H.; van Tol, M. F. H. *Organometallics* **1998,** *17*, 5222-5224.

29. Duchateau, R.; Cremer, U.; Harmsen, R. J.; Mohamud, S. I.; Abbenhuis, H. C. L.; van Santen, R. A.; Meetsma, A.; Thiele, S. K. T.; van Tol, M. F. H.; Kranenburg, M. *Organometallics* **1999,** *18,* 5447-5459.

30. Duchateau, R.; van Santen, R. A.; Yap, G. P. A. *Organometallics* **2000,** *19*, 809-816.

31. Yermiyahu, Z.; Landau, A.; Zaban, A.; Lapides I.; Yariv, S. *J. Thermal Analysis and Calorimetry* **2003,** *72*, 431-441.

32. Kiuchi, M.; Uchikawa, A.; Tanigmai, T.; Matsuzawa, S.; Yamura, K. *J. Appl. Polym. Sci.* **2002,** *85*, 632-637.

33. Kabalka, G. W.; Namboodri, V.; Akula, M. R. *J. Labelled Cpd. Radiopharm.* **2001,** *44*, 921-929.

34. Cui, Y.; Wang, M.; Chen, L.; Qian, G. *Dyes and Pigments* **2004,** *62*, 43-47.

35. Lye, J.; Freeman, H. S.; Cox, R. D. *Dyes and Pigments* **2000,** *47,* 53-64.

36. Neumann, B. *Dyes and Pigments* **2002,** *52*, 47-53.

37. Salem, I. A. *Transition Metal Chemistry* **2000,** *25*, 599-604.

38. Denizli, A.; Köktürk, G.; Salih, B.; Kozluca, A.; Pişkin. E. *J. Appl. Polym. Sci.* **1997,** *63*, 27-33.

39. Caerts, B.; Mol, V.; Sainte, T.; Wilms, G.; Van Den Berg, V.; Stessens, L. *Eur. Radiol.* **2001,** *7*, 474-476.

40. Anderson, S. A.; Frank, J. A.; *NMR Biomed.* **2007,** *20*, 200-215.

41. Biswas, S.; Hussain, S. A.; Deb, S.; Nath, R. K.; Bhattacharjee, D.; *Spectrochimica Acta Part A.* **2006**, *65*, 628-632.